The effects of topography around mountain foot on damage concentration

15 WCEE
LISBOA 2012

T. Maeda & T. Kimura
Dept. of Architecture, Waseda University, Tokyo, Japan

SUMMARY:
An earthquake of magnitude 6.7 occurred on a day after the tragic Tsunami earthquake in 2011, which jolted the central part of Japan and exerted tremendous damages in Sakae village. 25 completely collapsed houses and 69 partial collapsed houses were concentrated particularly in three areas in the village. These damages should primarily be attributed to its closeness to the causative fault; however, observable difference in damage level among and within these areas may be due to topography and subsurface structure. Micro-tremor measurements at single points and at triangular arrays enabled us to construct 3D topographic model with one layer over bedrock. 2D FEM simulation with an incident wave evaluated from nearby station record reveals relatively large ground motion on a cove along the river with concave mountain boundary, which matches relative severity in damage. It is concluded that nonlinearly elongated predominant period of soil and constructive wave interference should have contributed to the inhomogeneous damage pattern.

Keywords: Micro-tremor, Subsurface topography, Damage concentration, Rayleigh wave, 2D FEM

1. INTRODUCTION

An earthquake of magnitude 6.7 occurred on a day after the tragic Tsunami earthquake in 2011, which jolted the central part of Japan and exerted tremendous damages in Sakae village, fortunately with no death toll. Sakae village is a rural village known for deep snow accumulation, which hampered a detailed survey of earthquake damages right after the event. Three areas in the village, namely Mori, Aokura, and Yokokura were most severely damaged with 25 completely collapsed houses and 69 partial collapsed houses. These areas seem to be located right above the causative reverse fault, presumably on the upper block of it (NIED). The cause of these severe damages should primarily be attributed to its closeness to the fault; however, observable difference in damage level among and within these areas (Yamada et al.) may be due to topography and subsurface structure.

We have so far studied the effects of subsurface topography on damage concentration; for example, a small subsurface basin structure may have increased earthquake ground motion due to constructive wave interference and lead to small-scale damage concentration in Anamizu during the 2007 Noto-hanto earthquake (Shimizu et al., Shimizu & Maeda). Similar steps are taken to explain the aforementioned damage difference in Sakae village in view of small-scale subsurface anomaly around mountain foot. Our method is based on micro-tremor measurements and FEM simulation.

In the summer of 2011, we measured single point micro-tremor at 180 locations and micro-tremor triangular arrays at 2 locations in these areas. Servo type accelerometers with 256 Hz sampling and 16 bit resolution in about 3 Gal range were employed. Shear wave velocities of a surface layer and bedrock were deduced by simulating dispersion curves obtained by SPAC method, where peak frequencies of H/V spectra and boring data were referenced.

The distribution of peak frequencies of H/V spectra was utilized to construct a subsurface model of one surface layer over bedrock. All these areas are facing to the Chikuma River and bounded by mountain at the rear; Mori lies on an apron toward the river with relatively straight mountain boundary, while Aokura lies on a cove with concave mountain boundary. Surface layer is getting thicker unanimously toward the river in Mori, while surface layer is bounded in the direction parallel to the river in Aokura. In the most severely damaged area of Aokura, there is a certain damage distribution in the area. An incident wave was evaluated from nearby station record in Mori and used as input for 2D FEM simulation in Mori and Aokura. The simulation revealed relatively large ground motion in Aokura than in Mori and also inhomogeneous pattern of ground motion intensity in Aokura, which matches the relative severity of damage in that area.

2. DISTRIBUTION OF DAMAGE AND PREDOMINANT FREQUENCY

2.1. Fault mechanism and damaged area

An earthquake of magnitude 6.7 at the depth of 8km occurred on March 12, 2011 in the northern part of Nagano prefecture of Japan. A reverse fault mechanism was suggested by USGS and the distribution of small earthquakes reveals that areas of Mori, Aokura, and Yokokura in Sakae village are located right above the estimated fault plane by NIED as shown in Fig 2.1. Damage ratio of Aokura and Yokokura were estimated between 30% and 40%, while that of neighbouring Mori is less than 10 % (Yamada et al.). These areas are facing to the Chikuma River with mountains in the rear as shown in Fig. 2.2. Geologically, these areas had been formed by mudflow onto relatively firm Tertiary formation and impedance ratio at the interface seems to be high. The primary reason for severe damage in these areas should be the closeness to the fault plane; however, certain difference in damage level is observable.

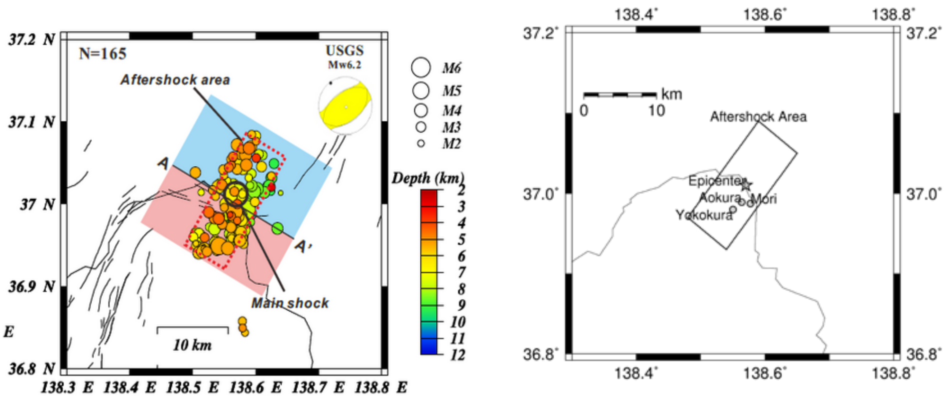

Figure 2.1. Fault mechanism and relative location of damaged areas (NIED)

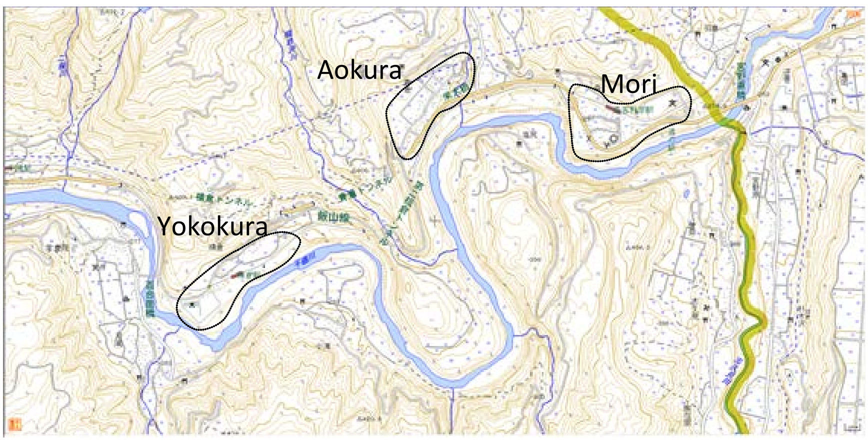

Figure 2.2. Location of damaged areas and topography around Sakae village

2.2. Distribution of predominant frequency

In the summer of 2011, micro-tremor was measured in Mori (72 points), Aokura (68 points), and Yokokura (40 points) by servo-type accelerometers in three components at each location. 10 minutes of acceleration was recorded with sampling frequency of 256 Hz, band pass filtered between 0.02Hz and 100 Hz. H/V spectra were evaluated by J-SESAME (Bard et al.) with stationary 20 second samples; root mean squared horizontal spectrum amplitude was divided by vertical spectrum amplitude and then averaged over samples.

Distributions of predominant frequency are depicted in Fig. 2.3. Mori looks like a flat apron sticking to the river and predominant frequency is decreasing to the west and toward the river. Relatively damaged part in Mori has predominant frequency around 4 Hz. Aokura looks like a flat concave cove and predominant frequency is decreasing toward the river and at the center of the cove. Center of Aokura was most seriously damaged and has predominant frequency around 3 Hz.

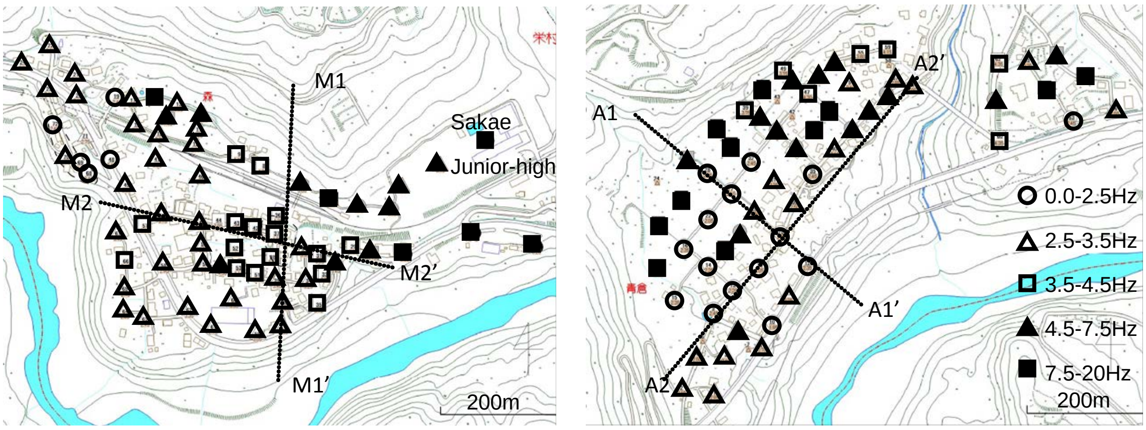

(a) Mori (b) Aokura

Figure 2.3. Distribution of predominant frequency

2.3. 1D model at the array site

Micro-tremor array measurements were carried out at Sakae junior high school at the east end of the Mori in Fig. 2.3a. An array constitutes four accelerometers for vertical component, one in the center and the other three evenly placed at the periphery of concentric circles of radii of 3m, 5m, 10m, and 20m. SPAC method was used to evaluate dispersion curves of surface waves. Fig. 2.4 shows dispersion curves, which suggests that the layer just below the surface would have phase velocity between 200m/s and 300m/s.

Boring data at the junior high school implies large impedance ratio at the depth of 8.5m. The dispersion curves were simulated by Rayleigh wave fundamental mode for bedrock overlain by a surface layer with constant surface layer thickness of 8.5m and appropriate shear wave velocity of surface layer and bedrock were sought to be 250m/s and 630m/s as shown in Tab. 2.1. Simulated dispersion curves in Fig. 2.4 reveal that this one-layer model can express basic feature of the array site. H/V ratio of Rayleigh wave fundamental mode trajectory shows similar frequency characteristics to H/V spectrum at the junior high school as shown in Fig. 2.5.

Table 2.1. Material properties for soil model

	Vs (m/s)	Vp (m/s)	Density (t/m^3)	Thickness
Surface layer	250	430	1.8	8.5
Bedrock	630	1180	1.8	-

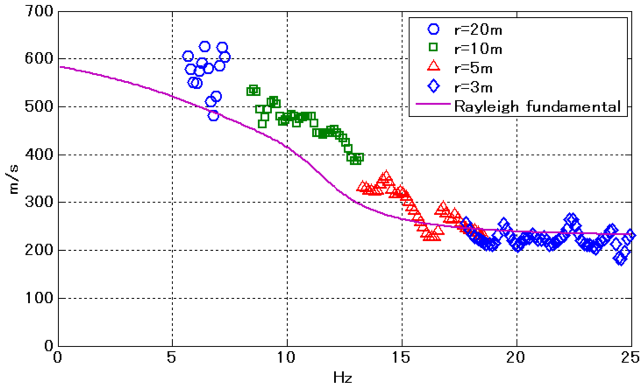

Figure 2.4. Dispersion curves at Sakae junior high school

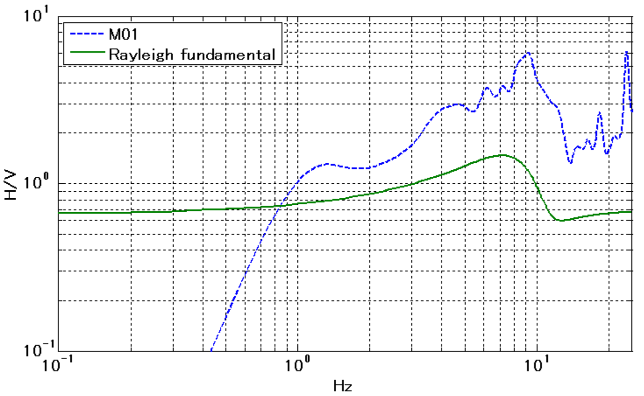

Figure 2.5. H/V spectrum at Sakae junior high school

2.4. Subsurface topography models

Predominant frequency of H/V ratio f can be related to surface layer thickness H by Eqn. 2.1, which is obtained by regression of frequency dependence of Rayleigh wave fundamental mode trajectory with material property shown in Tab. 2.1. This thickness corresponds to 1/4 wave length of shear wave of $Vs = 250 m/s$.

$$f = \frac{63}{H} = \frac{252}{4H} \tag{2.1}$$

Converting the distribution of predominant frequency to the distribution of surface layer thickness via Eqn. 2.1, we can construct 3D one-layer model for Mori and Aokura shown in Fig. 2.5. This figure shows contour lines of ground surface and distribution of surface layer thickness, where surface layer thickness in the mountain area was set to 3m referring to boring data at the mountain side of Mori. In Mori, surface layer is getting thicker toward west, from 8.5m at Sakae junior high school to more than 30m at the west end. In Aokura, surface layer is getting thicker toward the river, but has some irregularity implying shallow bedrock around the north end of the cove.

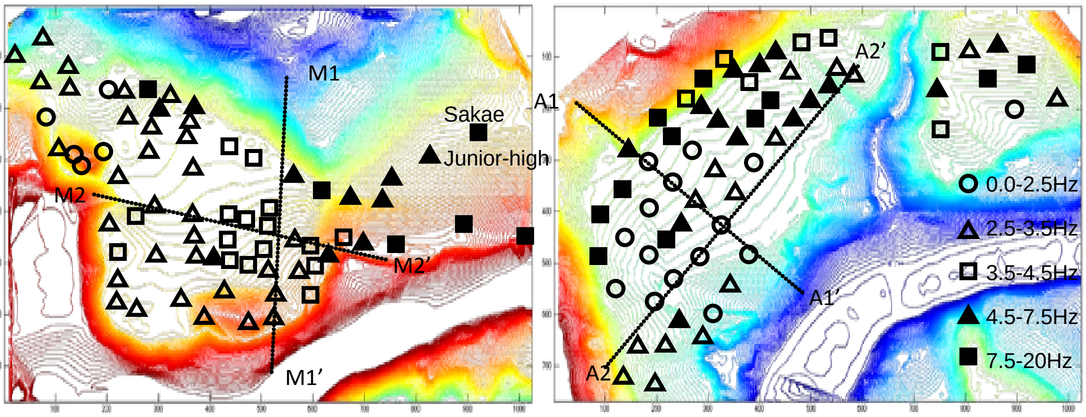

(a) Contour lines of ground surface (left: Mori, right: Aokura)

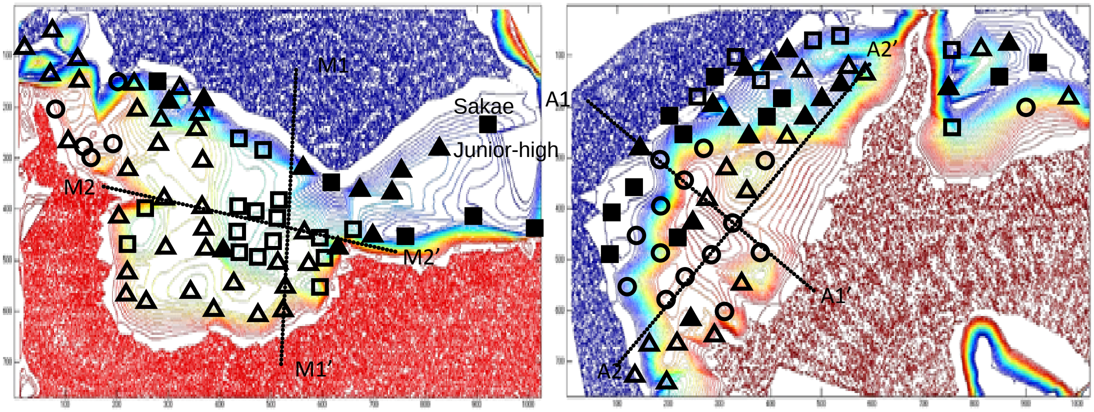

(b) Surface layer thickness (left: Mori, right: Aokura)

Figure 2.6. Contour for the surface and bedrock interface

2.5. 2D FEM models

2.5.1. Predominant frequency

By taking the section along relevant lines of damage in Fig. 2.3, 2D FEM models were constructed as shown in Fig. 2.8. Lines M1 and M2 pass through damaged area in Mori, while line A2 runs along the main street of Aokura intersected by line A1. Comparisons of FEM transfer functions, i.e. spectral ratio between ground motion and bedrock outcrop motion, and H/V spectra are exemplified for Aokura in Fig. 2.7. Frequency characteristics are similar at each location, revealing that deduced 2D FEM models retain their fundamental 1D frequency characteristics at each point.

2.5.2. Wave propagation characteristics

Basic wave propagation characteristics of these models were studied by applying Ricker wavelet for outcrop motion with representative center frequency of H/V predominant frequency of each model, namely 3.5Hz for M1 and M2 and 2.45Hz for A1 and A2. Wave traces are shown in Fig. 2.8 for each model. Model M1 and A1 are basically a section orthogonal to the river with thickening surface layer toward the river. Computed wave pattern show that direct wave is dominant at the mountain area. In the areas with sedimentation, reverberation and horizontally propagating wave from the mountain foot to the river are seen. Model M2 is basically horizontal layering and shows reverberation according to the distribution of surface layer thickness. Model A2 looks like an imperfect basin somewhat open to the east and exhibits reverberation and two-way horizontally propagating waves from each of the basin edge.

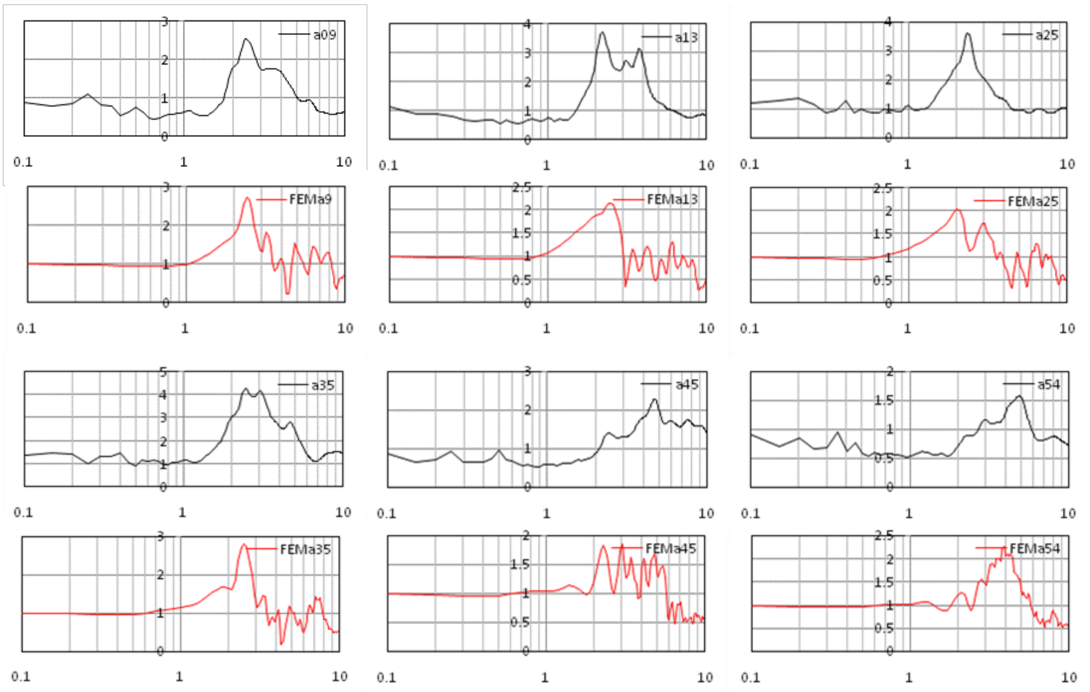

Figure 2.7. Frequency characteristics of FEM models and corresponding H/V spectra

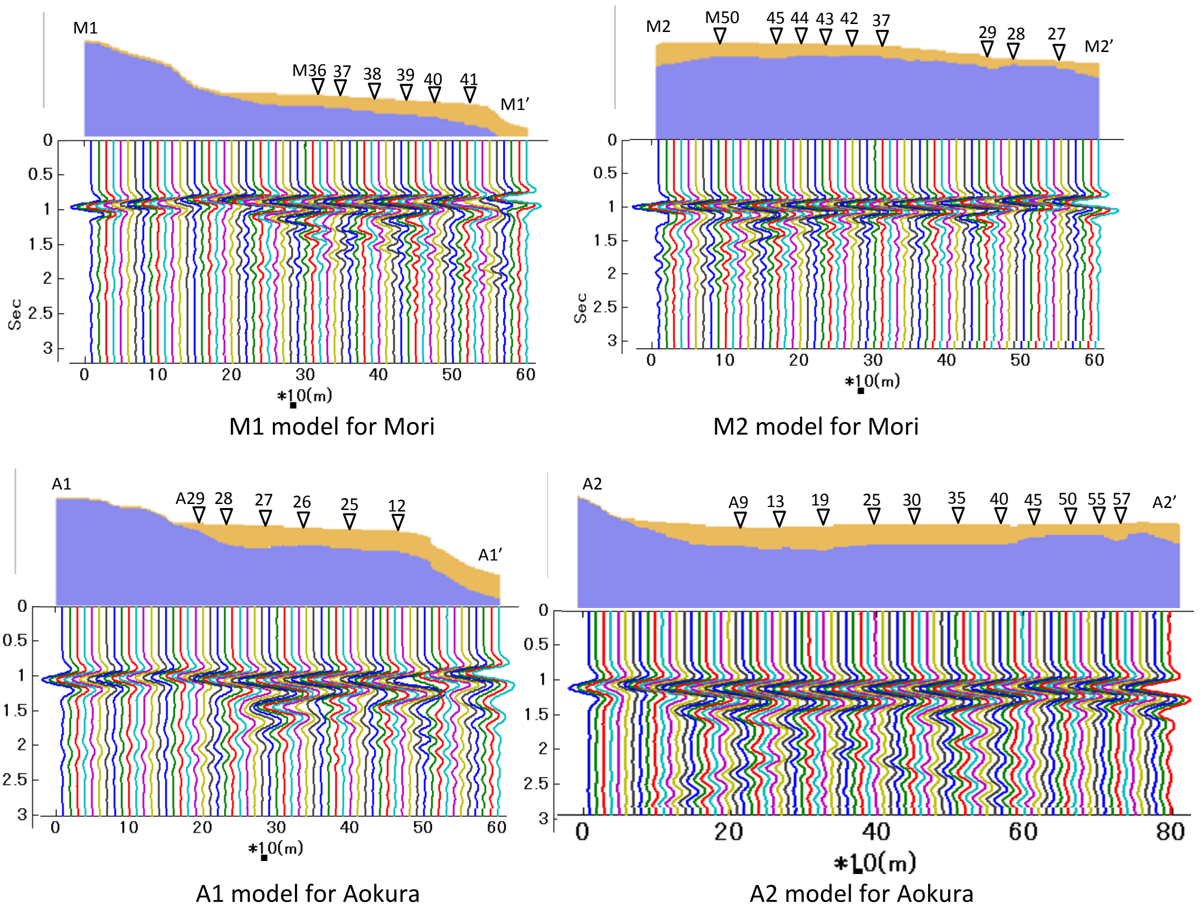

Figure 2.8. Wave propagation characteristics of FEM models

3. EVALUATION OF THE GROUND MOTION DURING THE MAIN SHOCK

3.1. Bedrock motion

Earthquake observation has been carried out at Sakae town office in the center of Mori by the government of Nagano prefecture and the main shock records have been distributed by SK-net. Acceleration time traces are shown in Fig. 3.1 and acceleration response spectra are in Fig. 3.2. Maximum acceleration is 9.47m/sec^2 in EW and 9.34m/s^2 in NS component. EW component shows separated two peaks at 0.49sec and 0.81sec, while NS component exhibits one major peak at 0.67sec.

Boring data at Sakae town office shows N-value constantly exceeding 50 below 19m, which is in parallel with surface layer thickness of 20m at an associated point in Model M1. Predominant frequency for stratum of 20m with Vs 250m/s is around 3Hz, which is similar to the H/V peak frequency around the office. Bedrock motion during the main shock is deduced from the records at the office by applying equivalent linear analysis on 1D wave propagation with an empirical strain dependence of modulus and damping proposed by Public Research Institute for gravel with constraining pressure of 335kPa as shown in Fig. 3.3, referring to experimentally obtained those relations from the observed records (Tokimatsu et al.). Maximum shear strain is as large as about 1%. De-convoluted EW outcrop motion is shown in Fig. 3.1 with its acceleration response in Fig. 3.2.

3.2. Evaluated ground motion

Equivalent linear analyses were carried out by the 2D FEM models with dynamic modulus reduction in Fig. 3.3. Acceleration wave traces are shown in Fig. 3.4 and velocity response spectra in Fig. 3.5, where solid lines are used to specify flat areas. Response around 1 sec to 2sec period is said to control damage of wooden houses (Sakai). These components for flat area in Mori are less pronounced compared to other models.

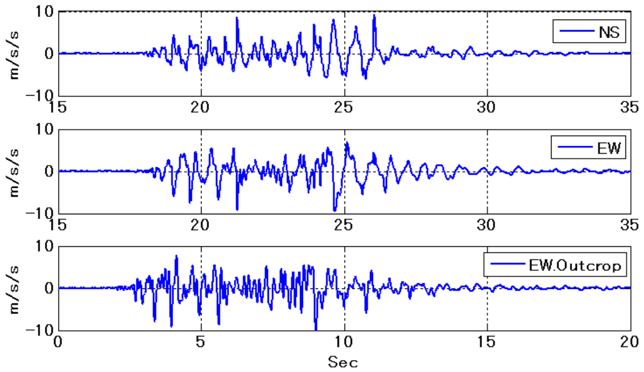

Figure 3.1. Acceleration time traces at Sakae village during the main shock and de-convoluted outcrop motion

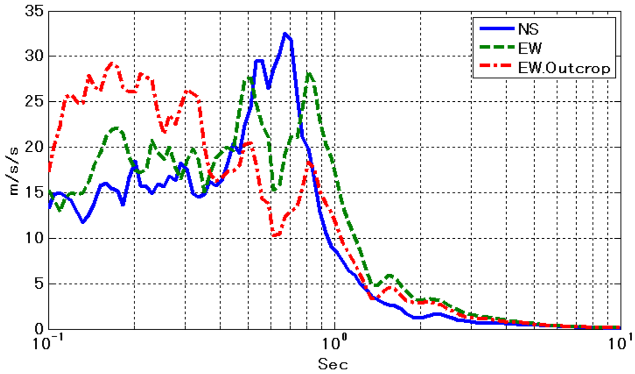

Figure 3.2. Acceleration response spectra in Sakae during the main shock and de-convoluted outcrop motion

In A1 model, these responses are unanimously large for flat area. In M2 model, response in these periods at flat area is decreasing toward east to less than 1.5m/s at 400m from the left edge where relatively severe damage was observed. In A2 model, response at 500m is most pronounced in flat area, where the damage was severest. This part is located just west to the shallow bedrock anomaly shown in Fig. 2.6.

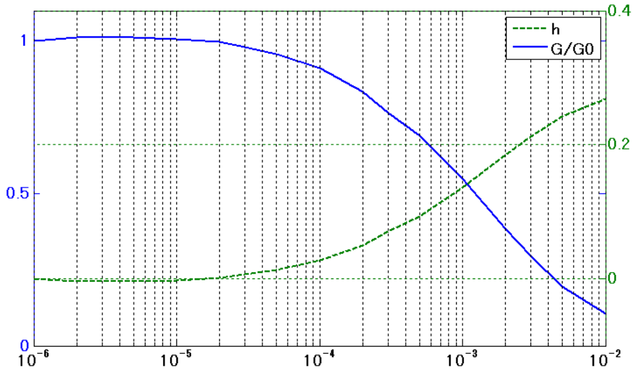

Figure 3.3. Modulus reduction ratio and damping dependence on strain

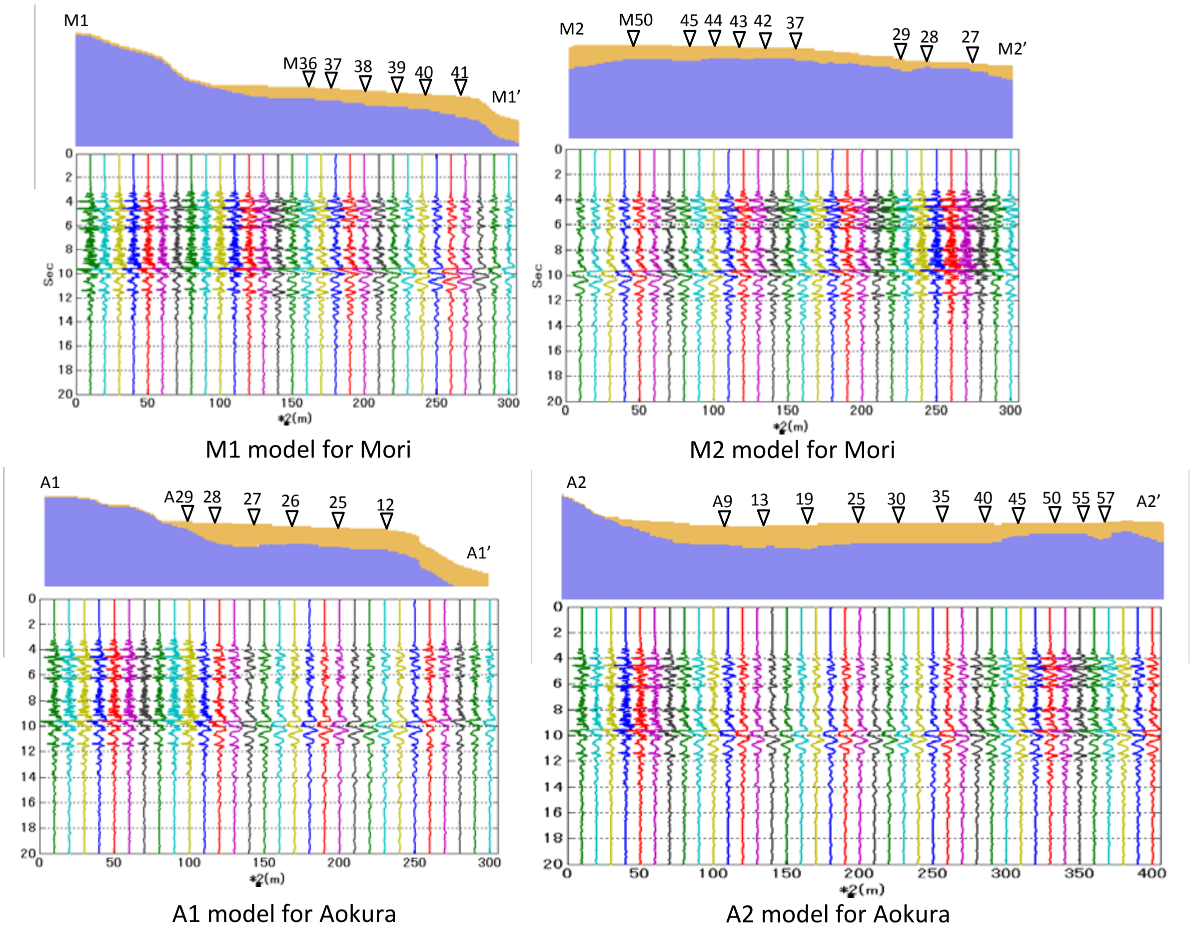

Figure 3.4. Distribution of acceleration time traces by equivalent linear 2D FEM

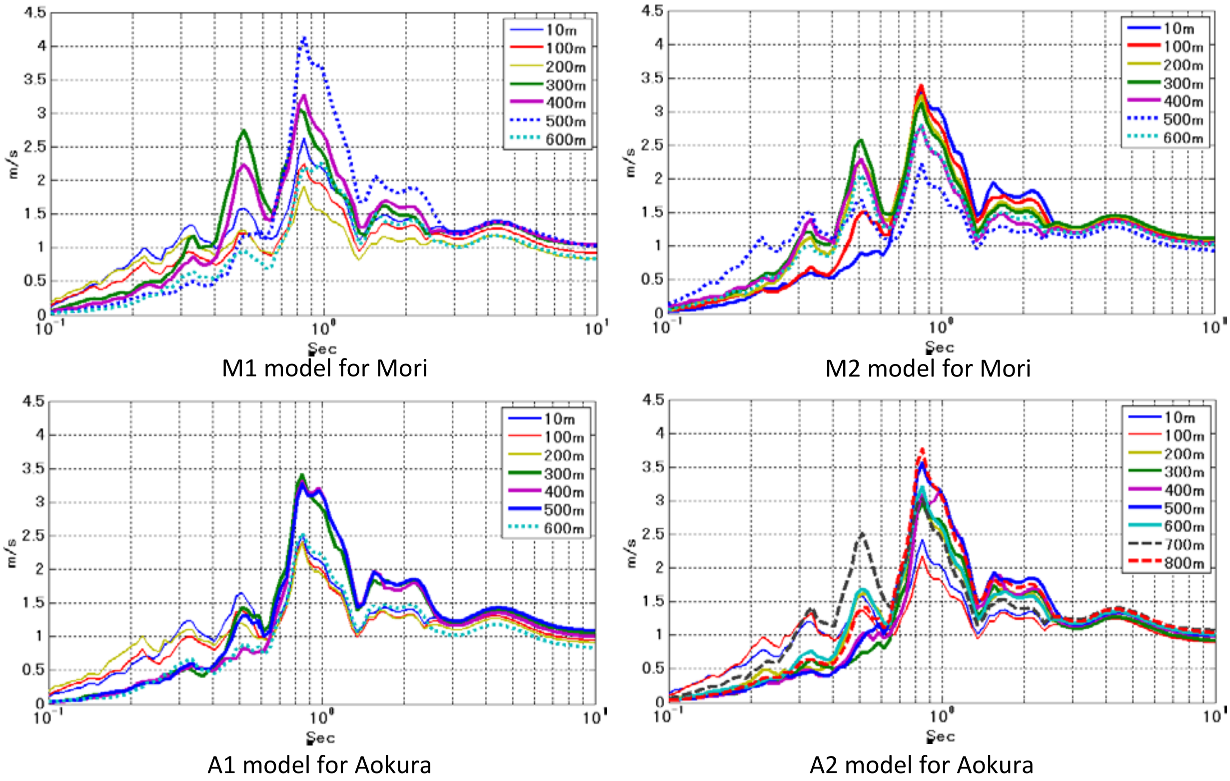

Figure 3.5. Velocity response spectra by equivalent linear 2D FEM

4. CONCLUSIONS

An earthquake of magnitude 6.7 exerted tremendous damages in Sakae village. The most severely damaged areas in the village, namely Mori, Aokura, and Yokokura seem to be located right above the causative reverse fault; however, observable difference in damage level among and within these areas were remarkable. We measured micro-tremor at single points and at triangular arrays. Shear wave velocities of a surface layer and bedrock were deduced by simulating dispersion curves. Distribution of peak frequencies of H/V spectra was converted to layer thickness of s surface layer, which turns into three dimensional topographic model of one layer over bedrock.

2D FEM models were extracted from the three dimensional topographic model. Wave propagation in these models is characterized by reverberation, surface wave generation, and interaction of these waves. An incident wave was evaluated from nearby station record in Mori and used for 2D FEM simulation of equivalent linear analysis. Simulation revealed relatively large ground motion at 1sec to 2sec period in damaged area in Aokura exceeding that in Mori, at those periods wooden houses are said to be most vulnerable. Inhomogeneous pattern of ground motion intensity in Aokura is also simulated. Most severely damaged area in Aokura is located next to the shallow bedrock anomaly at the north end of the cove.

Difference in damage level in small areas located along mountain foot can be characterized by FEM analysis based on micro-tremor measurements. Difference in responses are characterized by one dimensional reverberation with nonlinear period elongation and constructive wave interference of reverberation and surface wave generated at basin edges.

AKCNOWLEDGEMENT
We acknowledge SK-net for acceleration records in Sakae village acquired by Nagano prefecture government. We also acknowledge Sakae town office, Sakae elementary school, and Sakae junior high school for boring data and array measurements. We appreciate Mr. Atsushi Kato, an ex-graduate student for micro-tremor measurements. This work was partly supported by Grants-in-Aid for Scientific Research (21510298).

REFERENCES

Bard, P-Y. (2004). The Sesame Project: An overview and main results. 13th World Conference on Earthquake Engineering. #2207.

NIED (2011). http://www.hinet.bosai.go.jp/topics/n-nagano110312/

Sakai, Y. (2009). Reinvestigation on period range of strong ground motions corresponding to buildings damage, J. Struct. Constr. Eng., AIJ. **74:642**, 1531-1536. (Japanese).

Shimizu, R., Maeda, T., and Saito, G. (2008). Ground Motion Simulation in Anamizu Town during the 2007 Noto-Hanto Earthquake, Proc. Of 14th World Conference on Earthquake Engineering, **02**, #0154.

Shimizu, R. And Maeda, T. (2010). The effects of subsurface structure on the concentration of damage in town of Anamizu during the 2007 Noto-Hanto earthquake, J. Struct. Constr. Eng. AIJ., **75 :648**, 269-278, (Japanese).

Tokimatsu, K., Midorikawa S. and Yoshimi, Y. (1989). Dynamic soil properties obtained from strong motion records. Proc. 12th Intern. Conf. on Soil Mech. and Found. Eng.. **3**, 2015-2018.

Yamada, M. , et al. (2012). Estimation of Strong Motion and Building Damage Survey for the 2011 Northern Nagano Earthquake, Journal of JAEE, **12:1**, 20-30, (Japanese).